

Rubem P. Mondaini *Editor*

Trends in Biomathematics: Exploring Epidemics, Eco-Epidemiological Systems, and Optimal Control Strategies

Selected Works from the BIOMAT
Consortium Lectures, Rio de Janeiro,
Brazil, 2023



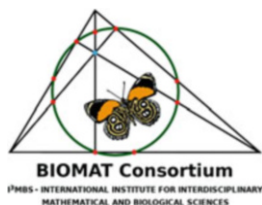
 Springer

Trends in Biomathematics: Exploring Epidemics, Eco-Epidemiological Systems, and Optimal Control Strategies

Rubem P. Mondaini
Editor

Trends in Biomathematics: Exploring Epidemics, Eco-Epidemiological Systems, and Optimal Control Strategies

Selected Works from the BIOMAT
Consortium Lectures, Rio de Janeiro,
Brazil, 2023



 Springer

Editor

Rubem P. Mondaini
BIOMAT Consortium
International Institute for Interdisciplinary
Mathematical and Biological Sciences
Rio de Janeiro, Brazil

Federal University of Rio de Janeiro
Rio de Janeiro, Brazil

ISBN 978-3-031-59071-9 ISBN 978-3-031-59072-6 (eBook)
<https://doi.org/10.1007/978-3-031-59072-6>

Mathematics Subject Classification: 92Bxx, 92-08, 92-10

© The Editor(s) (if applicable) and The Author(s), under exclusive license to Springer Nature Switzerland AG 2024

This work is subject to copyright. All rights are solely and exclusively licensed by the Publisher, whether the whole or part of the material is concerned, specifically the rights of translation, reprinting, reuse of illustrations, recitation, broadcasting, reproduction on microfilms or in any other physical way, and transmission or information storage and retrieval, electronic adaptation, computer software, or by similar or dissimilar methodology now known or hereafter developed.

The use of general descriptive names, registered names, trademarks, service marks, etc. in this publication does not imply, even in the absence of a specific statement, that such names are exempt from the relevant protective laws and regulations and therefore free for general use.

The publisher, the authors and the editors are safe to assume that the advice and information in this book are believed to be true and accurate at the date of publication. Neither the publisher nor the authors or the editors give a warranty, expressed or implied, with respect to the material contained herein or for any errors or omissions that may have been made. The publisher remains neutral with regard to jurisdictional claims in published maps and institutional affiliations.

This Springer imprint is published by the registered company Springer Nature Switzerland AG
The registered company address is: Gewerbestrasse 11, 6330 Cham, Switzerland

If disposing of this product, please recycle the paper.

Preface

Over the past four years, the conferences in the BIOMAT international series have had to adapt to the restrictions imposed on international conferences in an online format. Restrictions that proved even more severe for fully interdisciplinary conferences, such as our international symposia.

We often saw the participation of researchers and their students split into groups due to the existence of time zones. Were it not for the professionalism of the colleagues we know so well, it would have been even more difficult, sometimes impossible, to count on the participation of the vast majority, a fundamental condition for maintaining the top level of an interdisciplinary and multidisciplinary conference.

Very scarce financial resources made it impossible to organise hybrid sessions, with some support for PhD students and recent PhDs from developing countries. At all the conferences over the last four years, we have communicated to colleagues during the annual general meetings of our scientific association the decision to continue the mission of jointly organising this series of symposia. We are extremely grateful to all our colleagues. So many years of collaboration have created bonds of admiration and respect between us all.

This year, 2024, we hope to be able to organise our BIOMAT Symposium in person. Negotiations are underway to this end with the directors of the proposing institution. We will keep everyone informed and hope to continue counting on the support that the BIOMAT Consortium has always received.

The BIOMAT 2023 Symposium was held from November 6–9, 2023, and once again we had the support of the RNP/Brazil network and the cooperation of Dr. Beatriz Zoss, to whom we are once again very grateful on behalf of the BIOMAT Consortium. Our collaborators at the organisation's headquarters in Rio de Janeiro, Simão C. de Albuquerque Neto and Carmem Lucia S.C. Mondaini, provided invaluable help.

Rio de Janeiro, Brazil
November 10, 2023

Rubem P. Mondaini

Editorial Board of the BIOMAT Consortium

Adelia Sequeira	Instituto Superior Técnico, Lisbon, Portugal
Alain Goriely	University of Oxford, Mathematical Institute, UK
Alan Perelson	Los Alamos National Laboratory, New Mexico, USA
Alexander Grosberg	New York University, USA
Alexei Finkelstein	Institute of Protein Research, Russia
Ana Georgina Flesia	Universidad Nacional de Cordoba, Argentina
Alexander Bratus	Lomonosov Moscow State University, Russia
Avner Friedman	Ohio State University, USA
Carlos Condat	Universidad Nacional de Cordoba, Argentina
Denise Kirschner	University of Michigan, USA
David Landau	University of Georgia, USA
De Witt Summers	Florida State University, USA
Ding Zhu Du	University of Texas, Dallas, USA
Dorothy Wallace	Dartmouth College, USA
Eytan Domany	Weizmann Institute of Science, Israel
Ezio Venturino	University of Torino, Italy
Fernando Cordova-Lepe	Catholic University del Maule, Chile
Fred Brauer	University of British Columbia, Vancouver, Canada
Gergely Röst	University of Szeged, Hungary
Hamid Lefraich	University Hassan First, Morocco
Helen Byrne	University of Nottingham, UK
Jacek Miekisz	University of Warsaw, Poland
Jack Tuszynski	University of Alberta, Canada
Jane Heffernan	York University, Canada
Jerzy Tiuryn	University of Warsaw, Poland
John Harte	University of California, Berkeley, USA
John Jungck	University of Delaware, Delaware, USA
Karam Allali	University Hassan II, Mohammedia, Morocco
Kazeem Okosun	Vaal University of Technology, South Africa
Kristin Swanson	University of Washington, USA
Lisa Sattenspiel	University of Missouri-Columbia, USA

Louis Gross	University of Tennessee, USA
Lucia Maddalena	High Performance Computing and Networking Institute, ICAR - CNR, Naples, Italy
Luděk Berec	Biology Centre, ASCR, Czech Republic
Maria Vittoria Barbarossa	Frankfurt Inst. for Adv. Studies, Germany
Panos Pardalos	University of Florida, Gainesville, USA
Peter Stadler	University of Leipzig, Germany
Pedro Gajardo	Federico Santa Maria University, Valparaíso, Chile
Philip Maini	University of Oxford, UK
Pierre Baldi	University of California, Irvine, USA
Rafael Barrio	Universidad Autonoma de Mexico, Mexico
Ramit Mehr	Bar-Ilan University, Ramat-Gan, Israel
Raymond Mejía	National Institutes of Health, USA
Rebecca Tyson	University of British Columbia, Okanagan, Canada
Reidun Twarock	University of York, UK
Richard Kerner	Université Pierre et Marie Curie, Paris, France
Riszard Rudnicki	Polish Academy of Sciences, Warsaw, Poland
Robijn Bruinsma	University of California, Los Angeles, USA
Rubem P. Mondaini	Federal University of Rio de Janeiro, Brazil
Rui Dilão	Instituto Superior Técnico, Lisbon, Portugal
Samares Pal	University of Kalyani, India
Sandip Banerjee	Indian Institute of Technology Roorkee, India
Seyed Moghadas	York University, Canada
Siv Sivaloganathan	Centre for Mathematical Medicine, Fields Institute, Canada
Sándor Kovács	Eötvös Loránd University, Hungary
Somdatta Sinha	Indian Institute of Science, Education and Research, India
Suzanne Lenhart	University of Tennessee, USA
Vitaly Volpert	Université de Lyon 1, France
William Taylor	National Institute for Medical Research, UK
Yuri Vassilevski	Institute of Numerical Mathematics, RAS, Russia
Zhijun Wu	Iowa State University, USA

Contents

Mathematical Modeling of the Vaporization of Encapsulated Perfluorocarbon Nanodroplets Using Chirp Ultrasound: A Review	1
Kaiwen Jiang, Maryam Ghasemi, and Sivabal Sivaloganathan	
The Influence of Fear on Intraspecific Competition in Predator-Prey Dynamics: A Model-Based Study	33
Anal Chatterjee and Samares Pal	
Dynamical Study of a Predator-Prey Interaction Incorporating Fear Effect with Saturated Fear Cost and Prey Refuge	67
Anuj Kumar Umrao and Prashant K. Srivastava	
Optimal Control of HPV Infection and Cervical Cancer Cells with Beddington–DeAngelis Functional Response	89
Karam Allali	
On the Role of the Basic Reproduction Number in Systems Modeling Disease Propagation	105
Sándor Kovács and Szilvia György	
On a Discretized SIS Epidemic Model with No Vertical Transmission	123
Sándor Kovács and Noémi Gyúró	
Computational Modeling of Viral Infection and Immune Response in COVID-19 Patients	141
Hamid Lefraich	
Complex Dynamics of an Eco-epidemiological System with Fear and Allee Effect	169
Sasanka Shekhar Maity, Rakesh Medda, and Samares Pal	
Modeling the Dynamics of Vibrio-Phage Interactions: A Mathematical Approach	199
Anal Chatterjee and Suchandra Ganguly	

Waiting for the Perfect Vaccine	217
Gergely Röst, Zhen Wang, and Seyyed M. Moghadas	
In Silico Modeling of Antibiotics Treatment Combined with Corticosteroids for Septic Arthritis	233
Boróka Farkas and Nóra Juhász	
Epidemic Model for Risk-Based Testing and Quarantine	249
A. Dénes, G. Röst, and T. Tekeli	
Simple Case of Evolutionary Discrete Dynamics for Altruism with Reputation	261
Roberto Macrelli, Margherita Carletti, and Vincenzo Fano	
An Exploration of the Effects of Periodic Top Predator Interference and Hunting on a Predator-Prey System	277
Francesca Acotto, Leonardo Bardi, Alessandro Manzini, Olivia Sarfatti, Alberto Viscardi, and Ezio Venturino	
Modeling the Effect of Disease Characteristics on the Outcomes of Interventions	299
Cassandra Lisitza	
A Comprehensive Review of Sharma-Mittal Entropy Measures and Their Usefulness in the Study of Discrete Probability Distributions in Mathematical Biology	321
R. P. Mondaini and S. C. Albuquerque Neto	
Index	357

Epidemic Model for Risk-Based Testing and Quarantine



A. Dénes, G. Röst, and T. Tekeli

Abstract We construct and analyse a compartmental model for the spread of COVID-19 considering testing and quarantine with a risk-based evaluation of individuals to be tested, meaning that symptomatic individuals as well as contacts of confirmed cases are tested with higher probability. The model includes the isolation of the positively tested, for a fixed period of time, represented by a time delay in the differential equations. For a simplified version of the model we derive a final size relation, and we show that it approximates well the final epidemic size of the original model. Numerical simulations suggest that even a small improvement in identifying individuals with higher risk of being infected makes a testing program more efficient, having a significant impact on the mitigation of the epidemic.

1 Introduction

The COVID-19 epidemic started to emerge late 2019 and in a very short time went on to become a pandemic affecting all countries in the world. The emergence of a previously unknown virus has posed challenges for the health sector and decision makers, which had not been experienced in recent times. Before the first vaccines appeared, the most important way to slow down the spread of the disease was the application of non-pharmaceutical interventions including lockdowns, quarantine and isolation of infected individuals. The latter was made significantly more difficult by the fact that a huge fraction of infectious people remains symptomless and thus very hard to identify. Recognizing these infections and thus breaking chains of transmission is only possible by using tests. According to the WHO, diagnostic testing for COVID-19 has a critical role in the prevention and control strategy for COVID-19 and each country should have its own testing strategy that can be adapted to the actual epidemiological situation and the available resources [11].

A. Dénes · G. Röst (✉) · T. Tekeli

National Laboratory for Health Security, Bolyai Institute, University of Szeged, Szeged, Hungary
e-mail: denesa@math.u-szeged.hu; rost@math.u-szeged.hu; tekeli@math.u-szeged.hu

Several types of tests have been developed to identify COVID-19 infections. Nucleic acid amplification tests are the standard, while to achieve high coverage of testing, antigen-detection lateral flow or rapid diagnostic tests may also be applied as their application is simple and they provide rapid results. This improvement in the range of available testing methods which are more and more easy to perform enables their application in very large scales. According to the WHO, suspected individuals should always be prioritized for testing, especially in the case of lack of resources. More precisely, those who should be prioritized are people who are at risk of developing severe symptoms, health-care workers, inpatients in health-care facilities and the first symptomatic individual or subset of symptomatic individuals in a closed setting (e.g. long-term care facilities).

Most certainly, the above are not only true for the present pandemic, but also for future epidemics: one can expect that vaccines and medication will always take some time to develop and to run the clinical trials; hence, testing will be one of the first lines of defence in the fight against the spread of newly emerging diseases. Hence, while we include in our model some characteristic features of the ongoing COVID-19 epidemic (e.g. the latent and presymptomatic phase), the model is rather general and can be applied to other diseases as well.

The structure of the paper is as follows. In Sect. 2, we establish our model including mass testing and quarantine. In Sect. 3 we calculate the final size relation for a simplified model, which we use to approximate the final epidemic size (i.e. the total number of infections during the outbreak). In Sect. 4, we perform numerical simulations to study the efficiency of an increased testing of infected individuals. We also compare the numerical results concerning the final epidemic size with the estimates given by the final size relation deduced in Sect. 3. The paper is closed by a discussion.

2 Mathematical Model for Risk-Based Testing and Quarantine

We set up our base model as follows. We consider five subgroups of the population: susceptibles (denoted by $S(t)$); latent individuals, i.e. those who have already been infected but do not show symptoms and do not transmit the disease (denoted by $L(t)$); presymptomatic, i.e. those who do not show any symptoms yet but are already able to transmit the disease to a susceptible individual (denoted by $P(t)$); infectious (denoted by $I(t)$); and recovered (denoted by $R(t)$). The total population is denoted by $N(t)$. Transmission rate from the presymptomatic and the infected classes is denoted by β . Susceptibles, after infection, move to the latent class L . The total incubation time is assumed to be $\alpha_L^{-1} + \alpha_p^{-1}$ days, where α_L^{-1} is the length of time until becoming infectious and α_p^{-1} is the length of the presymptomatic period. Infectious individuals in class I need on average γ^{-1} days to recover and move to compartment R . There is an additional way of moving from each of the five

compartments considered in our model: a fraction of each compartment is moved to isolation based on a mass testing evaluated in the population. The notation σ_i with $i \in \{S, L, P, I, R\}$ stands for testing rates for the five compartments, while we apply the notations p_L, p_P and p_I for the sensitivity of the test, i.e. the probability that a test gives a correct positive result when applied to an infected individual from the compartment L, P or I , respectively. We denote by $1 - \rho$ the specificity of the test, i.e. ρ is the probability of the test giving a false-positive result in the case of a non-infected person being tested. After a confinement of τ days, individuals may return either to S or R , depending on whether a given individual being in isolation was correctly or falsely tested positive. Here we assume that all infected individuals recover at most in τ days; hence, all those who were actually infected can move to the recovered compartment. With the above notations and assumptions, our base model takes the form

$$\begin{aligned}
 S'(t) &= -\beta S(t)(I(t) + P(t)) - \rho\sigma_S S(t) + \rho\sigma_S S(t - \tau), \\
 L'(t) &= \beta S(t)(I(t) + P(t)) - \alpha_L L(t) - p_L\sigma_L L(t), \\
 P'(t) &= \alpha_L L(t) - \alpha_P P(t) - p_P\sigma_P P(t), \\
 I'(t) &= \alpha_P P(t) - \gamma I(t) - p_I\sigma_I I(t), \\
 R'(t) &= \gamma I(t) - \rho\sigma_R R(t) + p_L\sigma_L L(t - \tau) + p_P\sigma_P P(t - \tau) \\
 &\quad + p_I\sigma_I I(t - \tau) + \rho\sigma_R R(t - \tau).
 \end{aligned} \tag{1}$$

An additional auxiliary compartment may be considered to take account of those who are being in quarantine:

$$\begin{aligned}
 Q'(t) &= \rho\sigma_S S(t) + p_L\sigma_L L(t) + p_P\sigma_P P(t) + p_I\sigma_I I(t) + \rho\sigma_R R(t) \\
 &\quad - \rho\sigma_S S(t - \tau) - p_L\sigma_L L(t - \tau) - p_P\sigma_P P(t - \tau) \\
 &\quad - p_I\sigma_I I(t - \tau) - \rho\sigma_R R(t - \tau).
 \end{aligned}$$

For the total population $N(t) = S(t) + L(t) + P(t) + I(t) + R(t) + Q(t)$, we can easily see that $N'(t) = 0$; hence, the total population size is constant. Without loss of generality, upon variable rescaling we can normalize $N(t) = 1$, then the values of the model variables represent fractions of the population. Note that the equation for $R'(t)$ can be decoupled from the rest of the equations; hence, it is enough to consider the first four equations of model (1) and study the system

$$\begin{aligned}
 S'(t) &= -\beta S(t)(I(t) + P(t)) - \rho\sigma_S S(t) + \rho\sigma_S S(t - \tau), \\
 L'(t) &= \beta S(t)(I(t) + P(t)) - \alpha_L L(t) - p_L\sigma_L L(t), \\
 P'(t) &= \alpha_L L(t) - \alpha_P P(t) - p_P\sigma_P P(t), \\
 I'(t) &= \alpha_P P(t) - \gamma I(t) - p_I\sigma_I I(t).
 \end{aligned} \tag{2}$$

The basic reproduction number of model (2) expresses the expected number of secondary infections generated by a single infection in a susceptible population; in the absence of any control measure, in our situation this means all $\sigma_i = 0$. This can easily be calculated as

$$\mathcal{R}_0 = \beta(\alpha_p^{-1} + \gamma^{-1}),$$

given as the product of the transmission rate and the average infectious period (time spent in compartment P and I combined). The control reproduction number of model (2), counting the same quantity, but in the presence of control measures, can be calculated as

$$\mathcal{R}_c = \beta \frac{\alpha_L}{\alpha_L + p_L \sigma_L} \left(\frac{1}{\alpha_p + p_p \sigma_p} + \frac{\alpha_p}{\alpha_p + p_p \sigma_p} \cdot \frac{1}{\gamma + p_I \sigma_I} \right). \quad (3)$$

Here the term $\frac{\alpha_L}{\alpha_L + p_L \sigma_L}$ expresses the probability that an infected individual is not screened out during latency by testing before reaching the presymptomatic phase. Similarly, $\frac{\alpha_p}{\alpha_p + p_p \sigma_p}$ is the probability that a presymptomatic individual is not screened out and reached symptomatic phase. The terms $\frac{1}{\alpha_p + p_p \sigma_p}$ and $\frac{1}{\gamma + p_I \sigma_I}$ are the expected time durations spent in compartments P and I , respectively, taking into account the rates people are tested. Putting all together, \mathcal{R}_c is indeed the expected number of secondary infections in the presence of testing and isolation of positively tested individuals. We note that a similar model was studied in another study by the authors [7]; however, in that model various pooling strategies for the mass testing were also considered.

3 Final Size Relation for a Simplified Model

One of the key questions about an epidemic is the number of all infections during the whole epidemic period. Estimates for this value allow decision makers to plan ahead of time in questions regarding the epidemic. A final size formula is an analytic expression enabling us to predict the total number of infected during the course of the epidemic (for more details on final size relations, see, e.g. [1, 3–5]). In this section, we will calculate a final size relation for a special case of system (2).

To consider a simplified version of our model, we suppose that the specificity of the test is very high, i.e. no false-positive tests arise. This corresponds to $\rho = 0$. Then, model (2) is reduced to the following system:

$$\begin{aligned} S'(t) &= -\beta S(t) (I(t) + P(t)), \\ L'(t) &= \beta S(t) (I(t) + P(t)) - \alpha_L L(t) - p_L \sigma_L L(t), \\ P'(t) &= \alpha_L L(t) - \alpha_p P(t) - p_p \sigma_p P(t), \\ I'(t) &= \alpha_p P(t) - \gamma I(t) - p_I \sigma_I I(t). \end{aligned} \quad (4)$$

This reduced model is a system of ordinary differential equations; there is no explicit time delay anymore, which makes the analysis easier. To deduce the final size relation for system (4), we will need the following statements.

Proposition 1

- (i) All solutions of (4) that started from non-negative initial values will remain non-negative for all forward time.
- (ii) The infected compartments will eventually die out, i.e. $\lim_{t \rightarrow \infty} L(t) = \lim_{t \rightarrow \infty} P(t) = \lim_{t \rightarrow \infty} I(t) = 0$.
- (iii) The susceptible compartment tends to a positive limit as $t \rightarrow \infty$, i.e. $\lim_{t \rightarrow \infty} S(t) = S_\infty > 0$.

Proof

- (i) A general, well-known condition for preserving non-negativity of solutions of a system of ordinary differential equations $x'(t) = f(x(t))$ with $x(t) \in R^n$ and $f : R^n \rightarrow R^n$ is the following: for all i , $f_i(x) \geq 0$ whenever $x \geq 0$ (componentwise) and $x_i = 0$. In this case, if $x(t_0) \geq 0$ then $x(t) \geq 0$ for all $t \geq t_0$ for which it is defined. It is straightforward to check that (4) possesses this property. For example, if $L = 0$ and $S, P, I \geq 0$, then the right-hand side corresponding to L -equation is $\beta S(I + P) - \alpha_L L - p_L \sigma_L L \geq 0$. It is similar to other variables as well.
- (ii) From (i) it follows that $S(t)$ is non-increasing, since $S'(t) \leq 0$. By adding the first two, then first three and finally all four equations of (4), we can see that $S(t) + L(t)$, $S(t) + L(t) + P(t)$ and $S(t) + L(t) + P(t) + I(t)$ are all non-increasing functions from which, using the non-negativity of the four compartments, the boundedness of all four compartments follows.

From the boundedness and monotonicity of $S(t)$, we obtain that $S(t) \rightarrow S_\infty$ as $t \rightarrow \infty$ for some $S_\infty \geq 0$. Using this fact and the monotonicity and boundedness of $S(t) + L(t)$, one has $L(t) \rightarrow L_\infty$ as $t \rightarrow \infty$ for some $L_\infty \geq 0$, and proceeding in a similar manner, we obtain analogous statements for $P(t)$ and $I(t)$, i.e. all three infected compartments have a non-negative limit.

Let us first show that the I compartment dies out as $t \rightarrow \infty$. Suppose this is not true; hence, $I_\infty := \inf_{t \rightarrow \infty} I(t) > 0$. We have

$$\begin{aligned} (S(t) + L(t) + P(t) + I(t))' &= -p_L \sigma_L L(t) - p_P \sigma_P P(t) - p_I \sigma_I I(t) - \gamma I(t) \\ &< -\gamma I(t) < -\varepsilon \end{aligned}$$

for some $\varepsilon > 0$ for t large enough. From this it follows that $(S(t) + L(t) + P(t) + I(t)) \rightarrow -\infty$ as $t \rightarrow \infty$, which is a contradiction. The extinction of the other two infected compartments can be shown in an analogous way.

- (iii) $S(t)$ is non-increasing and bounded from below; hence, the statement follows using the fact that the total population is constant.

Theorem 1 *The final epidemic size of model (4) can be estimated using the final size relation*

$$S_\infty = S_0 e^{-\beta \frac{\alpha_P + \gamma + p_I \sigma_I}{\gamma + p_I \sigma_I} \frac{\alpha_L}{\alpha_P + p_P \sigma_P} \frac{S_0 - S_\infty}{\alpha_L + p_L \sigma_L}},$$

where $S_0 = S(0)$.

Proof For a compartment K of the model ($K \in \{S, L, P, I, R\}$), introduce the notations $K_\infty := \lim_{t \rightarrow \infty} K(t)$ and $\bar{K} := \int_{t=0}^\infty K(s) ds$. By integrating both sides of the equations for $P'(t)$ and $I'(t)$ of (4), we obtain

$$(\alpha_P + p_P \sigma_P) \bar{P} = \alpha_L \bar{L} \tag{5}$$

and

$$\alpha_P \bar{P} = (\gamma + p_I \sigma_I) \bar{I}, \tag{6}$$

while by adding the two equations for $S'(t)$ and $L'(t)$ and integrating both sides, we obtain

$$S_0 - S_\infty = (\alpha_L + p_L \sigma_L) \bar{L}. \tag{7}$$

From the first equation of (4), we have

$$S_\infty = S_0 e^{-\beta(\bar{I} + \bar{P})}. \tag{8}$$

From (5) and (7), we obtain

$$\bar{L} = \frac{S_0 - S_\infty}{\alpha_L + p_L \sigma_L} \quad \text{and} \quad \bar{P} = \frac{\alpha_L}{\alpha_P + p_P \sigma_P} \frac{S_0 - S_\infty}{\alpha_L + p_L \sigma_L}$$

and hence, using (6),

$$\bar{I} = \frac{\alpha_P}{\gamma + p_I \sigma_I} \frac{\alpha_L}{\alpha_P + p_P \sigma_P} \frac{S_0 - S_\infty}{\alpha_L + p_L \sigma_L}.$$

Substituting these expressions for \bar{P} and \bar{I} into (8), we obtain the implicit final size relation

$$S_\infty = S_0 e^{-\beta \frac{\alpha_P + \gamma + p_I \sigma_I}{\gamma + p_I \sigma_I} \frac{\alpha_L}{\alpha_P + p_P \sigma_P} \frac{S_0 - S_\infty}{\alpha_L + p_L \sigma_L}} \tag{9}$$

for S_∞ , which allows us to calculate an estimate for the final size of the susceptible compartment.

Let us remark that system (3) is a special case of the classical Kermack-McKendrick model, while (2) is not. Hence, we expect for (3) the classical final size relation

$$z = 1 - e^{-\mathcal{R}_0 z}$$

to hold, where z is the fraction of the immune population after the outbreak, in our case $z = (S_0 - S_\infty)/N \approx 1 - S_\infty$ (note also $S_0 \approx N = 1$). Notice that

$$\begin{aligned} & \frac{\alpha_L}{\alpha_L + p_L \sigma_L} \left(\frac{1}{\alpha_P + p_P \sigma_P} + \frac{\alpha_P}{\alpha_P + p_P \sigma_P} \cdot \frac{1}{\gamma + p_I \sigma_I} \right) \\ &= \frac{\alpha_P + \gamma + p_I \sigma_I}{\gamma + p_I \sigma_I} \cdot \frac{\alpha_L}{\alpha_P + p_P \sigma_P} \cdot \frac{1}{\alpha_L + p_L \sigma_L}, \end{aligned}$$

thus, comparing (3) and (9), we indeed find

$$z = 1 - e^{-\mathcal{R}_c z},$$

the standard final size relation with the basic reproduction number replaced by the control reproduction number. In what follows, we show that (9) approximates well the final epidemic size of the original model (2).

4 Numerical Simulations

4.1 The Control Reproduction Number as a Function of the Increased Testing Rates for Infected Individuals

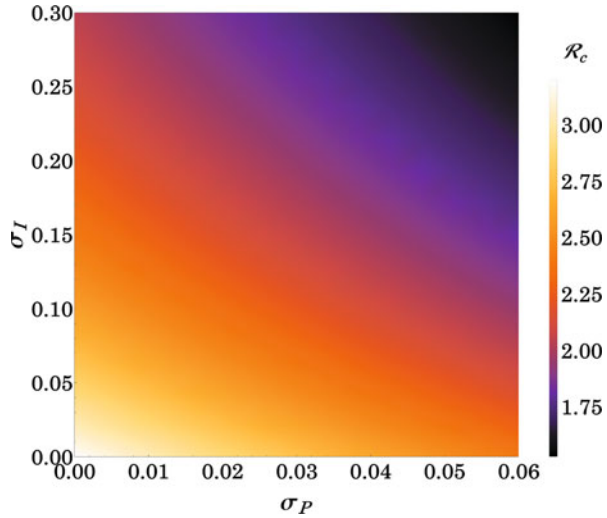
One of the most interesting features of our model is including the fact that in reality, not everyone gets tested with the same probability. Above all, infected people have a larger probability of being tested as several of them show symptoms. Latent and presymptomatic individuals may also have a higher probability of being tested, as they might be recognized as contacts of confirmed infected or might arrive from more affected areas, e.g. those coming home from holiday.

In Fig. 1, we can see the control reproduction number as a function of (σ_P) , the testing rate of presymptomatic individuals (those in compartment P) σ_I and the testing rate of symptomatic individuals (those in compartment I). The figure shows how efficiently an increased testing of infected individuals can reduce the number of the control reproduction number.

4.2 Effect of Increased Testing Probability for Infected Individuals

In this subsection, we perform numerical simulations to see the effect of an increased probability of being tested for latent, presymptomatic and infectious individuals. The simulations prepared for various values of σ_i ($i \in \{S, L, P, I, R\}$)

Fig. 1 The control reproduction number as a function of the testing rate of presymptomatic individuals (σ_P) and symptomatic individuals (σ_I). Other parameters are set to $p_L = p_P = p_I = 0.99$



and β (and hence the basic reproduction number), otherwise with the same parameters as above, are shown in Fig. 2. See Table 1 for an overview of the parameters. Note that model (2) is a system of delay differential equations with delay τ ; hence, for its numerical solutions an initial history function must be defined on the interval $[-\tau, 0]$. Since the R equation decouples it is sufficient to do this for S . For these scenarios, we assumed that testing started at $t = 0$; hence, for $t < 0$ nobody was in quarantine. This means that for $t \in [0, \tau]$, nobody returned to S from quarantine; hence, on this interval the system is equivalent with an ODE, and for $t > \tau$ the history function is given by the past solution.

We compare three scenarios concerning the basic reproduction number: a milder epidemic with $\mathcal{R}_0 = 1.8$, a more severe one where the reproduction number takes the value 3.2 and a very severe epidemic with $\mathcal{R}_0 = 6.5$. In all three scenarios, we compare four strategies for the testing of infected individuals: dark blue colour denotes the base situation when everyone gets tested with the same probability, while light blue, green and red curves are produced with a two, five and ten times higher probability of being tested for infected individuals, respectively. We can see that in each case, the introduction of measures like contact tracing and testing of those arriving from more affected areas, resulting in the infected being tested with a higher probability, will lead to a significant decrease of the peak of the epidemic and the total number of infected individuals. Depending on the value of the basic reproduction number, such interventions might even completely prevent an epidemic wave, allowing more time for preparation. In all cases, one can observe that introducing a higher probability of testing for the infected individuals, the peak of the epidemic is not only smaller but also shifted forward in time.

It should be noted, however, that it is not easy to quantify the probability of an individual being tested.

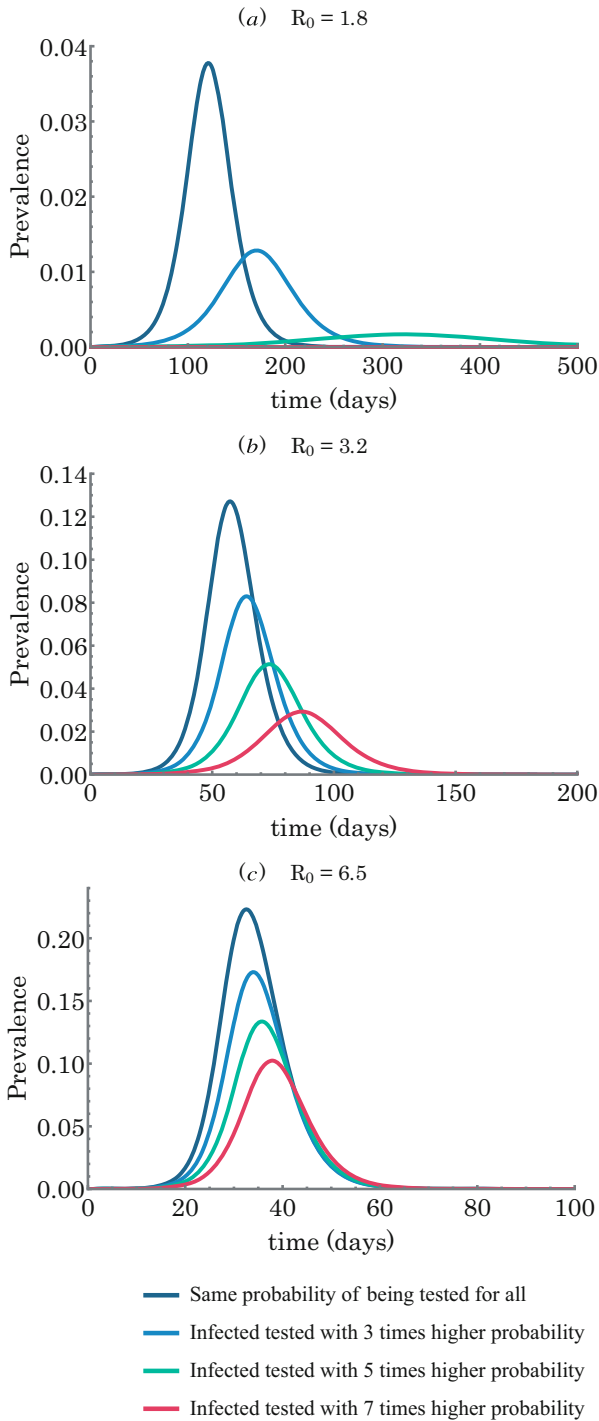


Fig. 2 Epidemic curves of model (2) with higher probability of infected being tested. The baseline testing rate is 0.02, and the four curves show a 3, 5 and 7 times higher probability of infected individuals (i.e. those in one of the compartments P , L , I) being tested compared to the baseline scenario of all individuals getting tested with the same probability

Table 1 Parameter description and values

Parameter	Description	Value	Source
\mathcal{R}_0	Basic reproduction number	1.8–6.5	–
β	Transmission rate	0.3–1.08	Calculated from \mathcal{R}_0
$1/\alpha_L$	Average time until infectiousness (days)	3.2	[10]
$1/\alpha_P$	Average time spent as presymptomatic (days)	2	[10]
$1/\gamma$	Length of infectious period (days)	4	[2]
p_L, p_P, p_I	Test sensitivity for latent/presymptomatic/infectious	0.5–0.99	[8, 9]
$1 - \rho$	Test specificity	0.95	[9]
τ	Length of isolation period (days)	14	[6]
$\sigma_i, i \in \{S, L, P, I, R\}$	Testing rate	0–1	Assumed

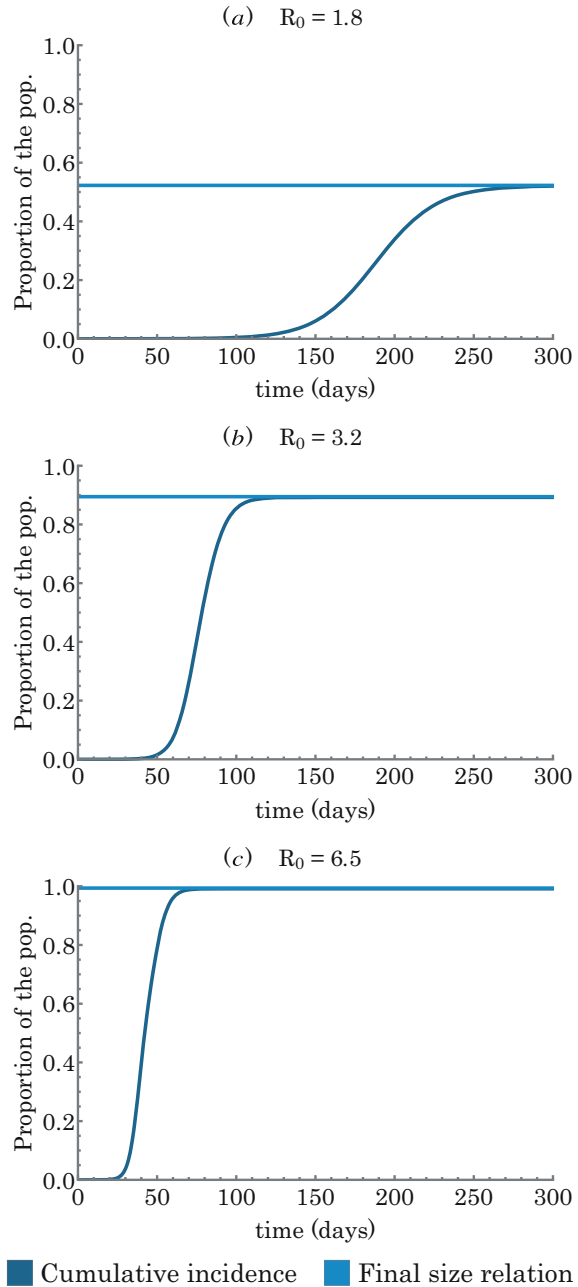
4.3 Final Size

In this subsection, we compare the final size of the epidemic obtained numerically from the simulations using various values for the basic reproduction number \mathcal{R}_0 and the final size estimation obtained using the analytic formula (9) deduced in Sect. 3. It should be noted that this formula is obtained for the simplified model (4) where 100% specificity was assumed and we considered $\sigma_S = \sigma_L = \dots = \sigma_R$, i.e. the same testing probability for all individuals. In Fig. 3, we can see that the estimation given by the final size relation forecasts well the final epidemic size in the case of equal probability of being tested in the whole population. As a comparison, we show the final epidemic size in the case of five times higher probability of being tested for the infected individuals. One can observe that in this case, the actual final epidemic size might be significantly lower than that forecasted by the final size relation. However, with an increasing value of the basic reproduction number, the final epidemic size increases even in this case; hence, the estimate becomes close to the actual value.

5 Discussion

In this paper, we have developed a compartmental model for COVID-19 transmission and mass testing-based isolation, considering susceptibles, exposed, presymptomatic, infected and recovered classes. The main novelty of the model is the inclusion of an increased probability of being tested for those who are actually infected. We have calculated a final size relation for a simplified version of the model. We have provided various numerical simulations to assess the possible positive effects of such an increased testing probability. The results of the simulations suggest that even a mild increase in the probability for infected individuals (being in various stages of infection) of being tested will result in a significantly more efficient

Fig. 3 Cumulative epidemic curves plotted along with the estimated final size, showing good agreement. Parameters are set to $\sigma_S = \sigma_R = 0.02$, $\sigma_L = \sigma_P = 0.03$ and $\sigma_I = 0.04$. The rest of the parameters are as shown in Table 1



testing program, while a sufficiently large (though, hardly achievable) difference in the probability of being tested could be able to completely eradicate the disease. This implies that such a simply executable change in the testing policy might turn out to be very helpful in reducing the total number of infections, and identifying individuals with a higher risk of being infected is an important component of test-trace-isolate strategies.

Acknowledgments A.D. was supported by the project No. 128363, implemented with the support provided from the National Research, Development and Innovation Fund of Hungary, financed under the PD_18 and FK_17 funding scheme. G.R. was supported by Hungarian grants NKFIH KKP 129877 and TKP2021-NVA-09. The authors were supported by RRF-2.3.1-21-2022-00006.

References

1. Arino, J., Brauer, F., van den Driessche, P., Watmough, J., Wu, J.: A final size relation for epidemic models. *Math. Biosci. Eng.* **4**, 159–175 (2007)
2. Ashcroft, P., Huisman, J.S., Lehtinen, S., Bouman, J.A., Althaus, C.L., Regoes, R.R., Bonhoeffer, S.: COVID-19 infectivity profile correction. *Swiss Med. Wkly* **150**, w20336 (2020)
3. Barbarossa, M.V., Dénes, A., Kiss, G., Nakata, Y., Röst, G., Vizi, Z.: Transmission dynamics and final epidemic size of Ebola Virus Disease outbreaks with varying interventions. *Plos One* **10**(7), e0131398 (2015)
4. Barbarossa, M.V., Bogya, N., Dénes, A., Röst, G., Varma, H.V., Vizi, Z.: Fleeing lockdown and its impact on the size of epidemic outbreaks in the source and target regions – a COVID-19 lesson. *Sci. Rep.* **11**, 9233 (2021)
5. Brauer, F.: A final size relation for epidemic models of vector-transmitted diseases. *Inf. Dis. Model.* **2**, 12–20 (2017)
6. Centers for Disease Control and Prevention, *Quarantine and isolation*, <https://www.cdc.gov/coronavirus/2019-ncov/your-health/quarantine-isolation.html>
7. Dénes, A., Röst, G., Tekeli, T.: Adaptive group testing in a compartmental model of COVID-19. *Math. Biosci. Eng.* **19**, 11018–11033 (2022)
8. Hellewell, J., Russell, T.W.: The SAFER Investigators and Field Study Team et al. *BMC Med.* **19**, 106 (2021)
9. Johns Hopkins Center for Health Security, *Serology-based tests for COVID-19* <https://www.centerforhealthsecurity.org/resources/COVID-19/serology/Serology-based-tests-for-COVID-19.html>
10. Moss, R., Wood, J., Brown, D., Shearer, F., Black, A.J., Cheng, A., McCaw, J.M., McVernon, J.: medRxiv 2020.04.07.20056184
11. World Health Organization, Recommendations for national SARS-CoV-2 testing strategies and diagnostic capacities, Interim guidance, 25 June 2021